Electrochemical CO2 reduction reaction on cost-effective oxide-derived copper and transition metal–nitrogen–carbon catalysts

Lin Zhang, Ivan Merino-Garcia, Jonathan Albo, Carlos Sánchez-Sánchez

Electrochemical CO_2 reduction reaction on cost-effective oxide-derived copper and transition metal-nitrogen-carbon catalysts

Lin Zhang[1], Ivan Merino-Garcia[2], Jonathan Albo[3], Carlos M. Sánchez-Sánchez*[1]

[1]*Sorbonne Université, CNRS, Laboratoire Interfaces et Systèmes Electrochimiques, LISE, 75005 Paris, France*

[2]*Associated Laboratory for Green Chemistry – Clean Technologies and Processes (LAQV), Chemistry Department, FCT, Universidade NOVA de Lisboa. 2829-516, Caparica, Portugal*

[3]*Department of Chemical & Biomolecular Engineering, University of Cantabria (UC), Avda. Los Castros 46, 39005 Santander, Spain*

* Corresponding author: carlos.sanchez@upmc.fr

Abstract

The electrochemical CO_2 reduction reaction (CO_2RR) either to generate multi-carbon (C_{2+}) or single carbon (C_1) value-added products provides an effective and promising approach to mitigate the high CO_2 concentration in the atmosphere and promote energy storage. However, cost-effectiveness of catalytic materials limits practical application of this technology in the short term. Herein, we summarize and discuss recent and advanced works on cost-effective oxide-derived copper (OD-Cu) catalysts for the generation of C_{2+} products (hydrocarbons and alcohols) and transition metal-nitrogen-doped carbon (M-N-C) electrocatalytic materials for C_1 compounds production from CO_2RR. We think they represent suitable electrocatalyst candidates for scaling up electrochemical CO_2 conversion. This short review may provide inspiration for the future design and development of innovative active, cost-effective, selective and stable electrocatalysts with improved properties for either the production of C_{2+} (alcohols, hydrocarbons) or carbon monoxide from CO_2RR.

Keywords:

Carbon dioxide electrochemical reduction reaction; Electrocatalysis; Oxide-derived copper catalysts; Transition metal-nitrogen-carbon catalysts; Value-added products

Introduction

The greenhouse gas carbon dioxide (CO_2) concentration in the atmosphere is sustainably increasing, leading to a monthly averaged value of 411.76 ppm recently, thus causing severe environmental impacts and energy issues.[1,2] Among the available CO_2 mitigation approaches, carbon capture and storage (CCS) and carbon capture and utilization (CCU) strategies are currently under development with the purpose of closing the anthropogenic CO_2 cycle [3–5]. The development of materials for efficient CO_2 capture is essential to facilitate a closed carbon cycle, nevertheless the focus of this article is on available technologies for converting CO_2 into value-added products.[6–9] In particular, electrochemical CO_2 reduction reaction (CO_2RR), which is powered by electricity, has attracted the scientific community attention for producing different fuel feedstocks such as carbon monoxide (CO) [10,11], formic acid (HCOOH) [12–14], methane (CH_4) [15,16], methanol (CH_3OH) [17,18], ethanol (CH_3CH_2OH) [19,20] and ethylene (C_2H_4) [21,22], etc. CO_2RR is mainly studied in aqueous media, however organic solvents and ionic liquids have also been explored.[23–25] The selectivity of this reaction is affected by different factors, such as the properties of both cathode electrocatalytic material and electrolyte, as well as the potential applied.[26–29] Moreover, another important aspect is the cell/electrolyzer design effect on productivity, selectivity and energy efficiency of CO_2RR. The simple undivided cell configuration has been replaced by two-compartment electrolyzers to avoid the reoxidation of reduced species. In addition to this, vapor-fed systems using gas diffusion electrode (GDE) and membrane electrode assembly (MEA or zero-gap assembly) configurations have been proposed to improve the transport of CO_2 to the catalyst surface, eliminating ohmic losses and thus maximizing energy efficiency [30,31].

Nowadays, efficient electrocatalytic materials with high electrocatalysis, strong stability and high product selectivity must be explored with the purpose of lowering the high overpotential of CO_2RR, avoiding also the effect of the competitive hydrogen evolution reaction (HER), which negatively affect the selectivity of the reaction toward the target product. In this context, different metallic electrocatalysts have been studied for CO_2RR, ranging from Cu (it seems to be the unique metal selective for

hydrocarbons and alcohols formation) [32,33] to Au, Ag, Zn (mainly producing CO)[34–36] and Pb, In, Sn, Bi (formate/formic acid generation).[13,37–39] Nonetheless, there are still many challenges to be addressed to reduce the overpotential and control the selectivity of CO_2RR on metallic electrocatalysts [40]. The main key parameters that need to be studied to improve both activity and selectivity are, among others, operating conditions (applied voltage, current density, catalyst loading, etc.) [41], electrolyte type and its concentration [26,42], local pH [43] and particle size [44].

From an industrial implementation point of view, generation of multi-carbon (C_{2+}) products (hydrocarbons and alcohols) from CO_2RR at Cu-based electrocatalysts represents an appealing approach because of their high energy density (used as liquid fuels) compared to C_1 feedstocks.[28,45] Nevertheless, Cu atoms mobility during CO_2RR (especially in the presence of CO) is well-known and provokes surface restructuring, which affects the electrode activity and product selectivity. For this reason, oxide-derived copper (OD-Cu) electrocatalytic materials have been widely studied in recent years, since OD-Cu electrodes provide better long-term stability under reaction conditions and keep a similar product selectivity [46]. Oxidation pretreatments on Cu electrodes can either increase surface roughness or provide subsurface oxygen at the electrocatalyst surface, which may lead to improve CO_2RR performance.[47–49]

Additionally, another interesting cost effective approach based on pyrolyzed catalysts for C_1 compounds production from CO_2RR, is reviewed in this work. In particular, transition metal-nitrogen-doped carbon (M-N-C) materials have been already studied for CO_2RR[50,51], HER[52] and Oxygen Reduction Reaction (ORR)[53,54] because of their high selectivity, stability and activity, huge catalytic surface area and low-cost. So far, generation of C_{2+} products from CO_2RR is not possible on M-N-C catalysts, since those are considered single active site catalysts and do not allow carbon-carbon coupling. Since Varela et al. reported the utilization of Fe/Mn-N-C for the first time on CO_2RR to CO with a Faradaic efficiency (FE) of 80% in 2015[55], there have been several attempts to explore different metals in M-N-C to catalyze CO_2RR such as Fe, Co, Ni, Mn, Cu, Cr, etc.[52,56,57] Among all these metals, Fe-N-C and Ni-N-C exhibit superior electrocatalysis by lowering the overpotential and improving CO selectivity, respectively.[56,58] Each component in M-N-C catalysts for CO_2RR may have a particular impact on the overall activity performance, since different types of carbon, nitrogen source and metallic

center have been explored.[59–61] However, most of the studies for CO_2RR have been mainly focused on the effect of different metallic centers in M-N-C catalysts.

To sum up, this work is mainly focused on the product-selectivity performance for CO_2RR on two types of cost-effective electrode materials, since we think they are feasible electrocatalytic material for real applications: i) OD-Cu catalysts for C_{2+} products formation, and ii) M-N-C materials for C_1 compounds production.

OD-Cu catalysts for multi-carbon products generation (alcohols and hydrocarbons)

Copper seems to be the unique metal which shows in literature the possibility of converting CO_2 into multi-carbon products (i.e. C_{2+} alcohols and hydrocarbons) with significant efficiencies.[62] Nevertheless, several drawbacks such as catalyst activity decrease during electrolysis and product selectivity limit the practical application of this technology in the short term. Different electrochemical and non-electrochemical oxidation pretreatments on Cu electrodes have been already tested to synthesize OD-Cu materials, since a relevant increase in grain boundaries and a rougher surface is created on those OD-Cu electrodes as soon as the required potential for CO_2RR is applied [63]. However, alterations in catalyst structure and morphology during CO_2RR may negatively affect the productivity and selectivity. Deactivation is mainly attributed to catalyst physical detachment due to HER, surface poisoning by adsorption of CO_2RR intermediates and/or restructuring of the electrode surface under reaction conditions.[64,65] This is not usually relevant when high surface area OD-Cu electrodes are used, otherwise it is an issue that must be addressed. In this regard, the continuous investigation on the CO reduction reaction mechanism, which is a key intermediate reaction to produce C_{2+} hydrocarbons and C_{2+} oxygenated products should help to move forward the development of alternative electrocatalysts and optimize operating conditions for CO_2RR. Furthermore, OD-Cu electrocatalytic materials selectivity for CO_2RR can also be tuned by the electrolyte. In particular by controlling the buffer capacity, local pH, anion and cation of the supporting electrolyte in solution [26,42,43]. Neutral unbuffered and alkaline aqueous solutions favor formation of C_{2+} over C_1 products on OD-Cu electrodes. For this reason, oxidation-reduction cycles at the OD-Cu electrodes, which create a higher roughness electrode surface, lead to a higher local pH close to the electrode surface, which enhances C_{2+} products formation. Additionally, electrolyte anions and cations play a critical role in the CO_2RR selectivity

towards C_{2+} products, being Cs^+ as alkali cation and halides as anions the most active electrolytes for that purpose.

Herein, we summarize recent research on OD-Cu electrocatalysts with high catalytic efficiency and activity (Table 1). Since Frese et al. firstly reported that OD-Cu electrodes can be used to convert CO_2 to methanol in aqueous solution, [66] several authors have extensively investigated the use of OD-Cu surfaces in CO_2RR for alcohols production. For instance, the treatment of Cu_2O with Prussian Blue analogue (K-PBA) to form core-shell nanocubes (Cu_2O@K-PBA) increases C_{2+} products yields with FE of 23.9% (ethylene 10.8%, ethanol 3.6% and n-propanol 9.5%) due to the ability of K-PBA for changing the intrinsic energetics of Cu_2O.[67] From another point of view, theoretical methods such as the density functional theory (DFT) may provide a new approach to study reaction mechanisms of CO_2RR-to-methanol process on Cu_2O. [68] Thus, DFT was used to investigate the formation of the helpful reaction intermediate CH_3OH*-OH*, as well as figuring out the influence of catalyst surface morphology and solvation during methanol formation from CO_2RR. Furthermore, the authors also strengthened the "variation trend of charge distribution", leading to the choice of "minimum-energy pathway".

Likewise, a lot of efforts have been also dedicated to develop and improve OD-Cu electrocatalysts for CO_2RR to produce C_{2+} hydrocarbons. For instance, Boron-doped OD-Cu greatly catalyze CO_2 to C_2 products owing to the impact of Boron on stabilizing Cu^+ species. [69] In this regard, the effect of Zn on stabilizing Cu^+ atoms as well as suppressing H_2 evolution in Cu oxides/ZnO-based electrocatalytic surfaces for the production of hydrocarbons from CO_2RR was also illustrated, leading to an outstanding performance toward ethylene with FE as high as 91.1%, which the authors associated to the synergic effect between Cu oxides and ZnO, with improved adsorption of reaction intermediates for the generation of ethylene. [70] Similarly, N-doped carbon (N_xC) was adopted as a carrier of CuO by catching more CO_2 to increase ethylene selectivity. Compared to CuO loaded onto carbon black, the former shows better ethylene selectivity and activity. This research provides an efficient method to increase catalytic activity and reaction selectivity by combining CuO and CO_2 capture materials.[71] In addition, the utilization of ionic liquid functionalized graphite sheets was also studied for controlling the morphology and size of Cu_2O nanocubes (Cu_2O/ILGS).[72] Cu_2O/ILGS are able to inhibit the latter's aggregation, thus enlarging the surface active sites for CO_2RR and reaching a high ethylene efficiency

(Fig 1a). Moreover, OD-Cu catalysts may modify their morphology during CO_2RR. For example, Cu_2O nanoparticles can undergo fragmentation to smaller pieces during the electrochemical process, thus increasing compact morphology and grain boundaries, which may facilitate the selectivity and activity toward C_{2+} products.[73] Fig.1b shows a typical OD-Cu electrode morphology with numerous grain boundaries. In particular, grain boundaries play a crucial role for faster oxygen diffusion and oxide nucleation in OD-Cu catalyst. The high presence of grain boundaries in the catalyst structure is responsible for promoting the formation of C_2/C_3 products.[74][75] Interestingly, the major impact of applied potential and current on reaction selectivity at OD-Cu catalysts was proven.[76] The authors prepared 3 different kinds of OD-Cu films with different surface roughness factors and illustrated that product selectivity relies on surface roughness: methane, ethylene, ethanol, CO or formate generation can be improved successively as the OD-Cu films surface roughness aggravates. As shown in Fig. 1c, 1d and 1e, the control of the applied potential (ranging from -0.45V to -1.3 V vs. RHE) is crucial to tailor the selectivity of CO_2RR. The different products are related to the different energy barriers in the CO_2RR process. For instance, a slightly rough metallic Cu surface (Cu-10) produces preferentially CH_4 while OD-Cu surfaces (CuO-1, CuO-10 and CuO-60) produce more C_2H_4 and C_2H_5OH. In addition to this, the method of isotopic labelling, which can trace the products composition and uncover the reaction mechanism by supplying isotopic reactant, provides information to understand product distribution during CO_2RR. This method can be used for the correct identification of active sites in electrocatalysis, that is, the specific facet/feature on the catalyst surface where CO_2RR to form the target product is taken place.[77] For instance, given a mixture of ^{13}CO and $^{12}CO_2$, three different existing actives sites were identified for different C-C coupled products formation from CO_2RR at OD-Cu catalysts such as ethylene, ethanol/acetate and 1-propanol, respectively.

Transition Metal-Nitrogen-Carbon materials for single carbon products generation

As mentioned above, OD-Cu materials mainly boost the catalytic activity for promoting the formation of C_{2+} products. For CO generation, however, M-N-C catalysts (Fig. 2a) have been widely studied in literature due to their numerous active sites of synergistic M-N_x moieties on their huge surface area, which might modify the binding energy of key reaction intermediates related to CO_2RR. Unfortunately, these transition metals have excellent and prior catalysis on competing side HER rather than CO_2RR. However, when metal arrangement goes into a single atom structure, its electrocatalytic role on CO_2RR

can be greatly enhanced due to the electronic environment, which has received a lot of attention recently.[60] The comparison of CO faradaic efficiencies (FEs) at different metals-N-C electrocatalysts as a function of the applied potential is shown in Fig.2b. The highest CO production efficiency is exhibited by Ni-N-C, but the lowest overpotential is achieved by Fe-N-C catalyst. For these reasons, we focus this section in Fe-N-C and Ni-N-C catalysts for CO_2RR. The identification of single active sites on those catalyst depends on each case, since the nature of the metal center and its coordination environment define different types of active sites (M-N, M-C, M-N_{2+2}, M-N_4-C…), which mainly control activity and selectivity in M-N-C catalysts.[50] For instance, the utilization of porous nanosphere Fe-N-C for CO_2RR to CO shows an interesting high FE (around 90%), where the key aspect in terms of active sites was demonstrated to be the synergistic role between the single-atom Fe-N_4 moieties and adjacent C [78]. In addition, rotating disk electrode (RDE) was used to carry out linear sweep voltammetry (LSV) analyses in order to measure the electrochemical response in the presence or absence of Fe center (Fig.2c). In this regard, the presence of Fe center notably enhances the catalytic performance despite nitrogen moieties are already catalytically active for CO_2RR. This leads to the conclusion that the Fe atom plays a vital role in the active sites of the electrocatalytic material for an efficient CO_2RR. In this context, DFT calculations were used to evaluate the nature of real active sites in this type of electrocatalyst. It was proven that the most active sites are the Fe-N_4 moieties surrounded by defective graphitic carbon, because this kind of moieties possesses the smallest Gibbs free energy (Fig.2d). Surprisingly, this research reports an extremely small overpotential of 90 mV, which is the lowest reported for Fe-N-C catalysts.[79]. Zhou et al. stated that Fe-N-C materials derived from $Fe(SCN)_3$ (denoted as SMFeSCN) are responsible for an improved FE to CO up to 99% at a moderate overpotential of 0.44 V, in comparison with the performance reached on SMFe (without SCN). Nevertheless, this enhancement was mainly attributed to the 3D graphene microporous nanostructure of SMFeSCN, which leads to an increased CO_2 local concentration.[80] Another strategy following this approach is based on sulfur (S) incorporation in the Fe-N-C synthesis for producing numerous micropores and high surface area electrodes, which reach an enhanced FE for CO generation of 98%.[81] The dopant S is embedded in the graphitic layer together with Fe-N_4, thus increasing the activity of the latter by changing its Fermi level and charge density (Fig.2e and 2f).unlike Fe-N-C catalysts, which are beneficial for lowering the overpotential for CO formation, Ni-N-C materials are popular mainly because of their high CO

selectivity. This fact is mainly attributed to the presence of Ni single atoms within the Ni-N-C electrocatalysts.[60] Based on this, we summarize here the proposed active sites present on those catalysts, which justify high FEs to CO achieved on Ni-N-C electrocatalysts. The combination of experimental and DFT calculations proved that N and C surrounding Ni atoms can help the transportation of electrons through Ni d orbital to reactants and lower the energy [82]. In principal, the most important active sites are located in the Ni-N_x moieties, which can act either in a synergistic way with different N or be affected by the surrounding environment. For instance, two different groups of research have demonstrated the importance of pyrrolic N in the synergistic effect with Ni-N_x by controlling nitrogen precursors in an attempt to tune the catalytic activity for FEs of 96.5% and 80% to CO, respectively. [83] [84] In addition to this, different Ni-N_x moieties can be found depending on the number and species of N and the surrounding environment, causing different catalytic activities. As a result, DFT is used to analyze the most valuable active site Ni-N_x.[85,86] In this regard, the free energies of the intermediate *COOH on different Ni-N-doped carbon nanotubes such as Ni@N_3 (pyrrolic), Ni@N_3 (pyridinic) and Ni@N_4, respectively, were calculated [85]. Ni@N_3 (pyrrolic) was the most efficient active site due to its lowest free energy (Fig. 3a). Moreover, rhombic dodecahedron shape of Ni-N-C was also developed in order to compare the behavior of this catalysts in the presence/absence of the metal center (Ni). Thus, Ni-N-C showed better electrocatalysis than N-C catalyst in terms of high FE toward CO (Fig.3b) and more positive onset potential (Fig.3c). Nevertheless, the authors found out that Ni-N_4 (Ni-N_4-C_{10}) matters in the catalysis reaction, that is, in other words, the edge-located Ni-N_{2+2} (Ni-N_{2+2}-C_8) is responsible for the high selectivity to CO (96% FE) rather than Ni-N_4 in bulk Ni-N-C rhombic dodecahedron (Fig.3d).[86] These conclusions may provide new insights into the synthesis of specific Ni-N-C electrocatalysts with desired properties for an improved CO_2RR-to-CO process efficiency and selectivity. In conclusion, M-N-C catalysts are promising low-cost catalytic materials for CO generation from CO_2RR due to their enhanced electrocatalytic activity compared to metal-free N-doped carbon materials, especially Fe-N-C and Ni-N-C catalysts, which shown excellent performance for converting CO_2 to CO with high FEs.

Conclusions

In summary, the most recent trends on cost-effective OD-Cu catalysts and M-N-C materials for the CO_2RR in aqueous media are reviewed here. On the one hand, different operating conditions (pH, electrolyte, applied potential etc.) as well as electrode morphology control and increased surface roughness seem to dramatically enhance the performance of CO_2RR to C_{2+} products (alcohols and hydrocarbons) in terms of reaction selectivity and catalyst activity. In our opinion, most of the future research on OD-Cu catalysts should be focused on continuing the study of the CO reduction reaction mechanism, which is a key intermediate reaction to produce C_{2+} hydrocarbons and C_{2+} oxygenated products on OD-Cu catalysts. On the other hand, pyrolyzed catalysts for C_1 compounds production (mainly CO) such as Fe-N-C and Ni-N-C materials have already demonstrated an outstanding FE to convert CO_2 into CO at low overpotentials. Some controversy is present in the identification of the real active sites on those materials. Most of the reported studies agree in the nature of the metal center and its coordination environment with the surrounding nitrogen and carbon atoms as the main active sites. Nevertheless, the long-term stability of M-N-C materials is still an issue, since relevant leaching of the metal center is produced under reaction conditions during CO_2RR. For this reason, we suggest to concentrate future research developments on that. Finally, this short review may provide new insights for the future development of cost-effective, selective, and stable electrocatalysts for an improved CO_2RR performance toward the generation of different types of value-added products.

Conflict of interest statement

The authors declare no interest conflict.

Acknowledgements

C. M. Sanchez-Sanchez thanks the funding of Sorbonne Université - China Scholarship Council program 2017 and Labex Matisse program (ASDB/2017-12) for the PhD contract of L. Zhang, as well as the ECOS Sud-Chile CONICYT program (Project C17E10). Thanks for the help of Dr. F. J. Recio Cortes and Dr. R. Venegas in Pontificia Universidad Católica de Chile. I. Merino-Garcia would like to thank his Post-doctoral contract in the frame of Research Project PTDC/EQU-EPQ/29579/2017, financed by “Programa Operacional Regional de Lisboa, na componente FEDER” and “Fundação para

a Ciência e Tecnologia, I.P.". J. Albo gratefully acknowledge the Spanish Ministry of Economy Competitiveness (MINECO) under Ramón y Cajal program (RYC-2015-17080).

References and recommended reading

Papers of particular interest, published within the period of review, have been highlighted as:

* of special interest

** of outstanding interest

1. Earth System Research Laboratory: **Global greenhouse gas reference network: trends in atmospheric carbon dioxide**. *Glob Greenh Gas Ref Netw* 2019,

2. Cox PM, Betts RA, Jones CD, Spall SA, Totterdell IJ: **Acceleration of global warming due to carbon-cycle feedbacks in a coupled climate model**. *Nature* 2000, **408**:184–187.

3. Davis SJ, Lewis NS, Shaner M, Aggarwal S, Arent D, Azevedo IL, Benson SM, Bradley T, Brouwer J, Chiang YM, et al.: **Net-zero emissions energy systems**. *Science* 2018, **360**:9793.

4. Sgouridis S, Carbajales-Dale M, Csala D, Chiesa M, Bardi U: **Comparative net energy analysis of renewable electricity and carbon capture and storage**. *Nat Energy* 2019, **4**:456–465.

5. Zhang W, Hu Y, Ma L, Zhu G, Wang Y, Xue X, Chen R, Yang S, Jin Z: **Progress and perspective of electrocatalytic CO_2 reduction for renewable carbonaceous fuels and chemicals**. *Adv Sci* 2018, **5**:1700275.

6. Kibria MG, Edwards JP, Gabardo CM, Dinh C-T, Seifitokaldani A, Sinton D, Sargent EH: **Electrochemical CO_2 reduction into chemical feedstocks: from mechanistic electrocatalysis models to system design**. *Adv Mater* 2019, **31**:1807166.

7. Garg S, Li M, Weber AZ, Ge L, Li L, Rudolph V, Wang G, Rufford TE: **Advances and challenges in electrochemical CO_2 reduction processes: an engineering and design perspective looking beyond new catalyst materials**. *J Mater Chem A* 2020, **8**:1511–1544.

8. Hussin F, Aroua MK: **Recent advances in low-temperature electrochemical conversion of carbon dioxide**. *Rev Chem Eng* 2020, **1**:https://doi.org/10.1515/revce-2019-0010.

9. Weekes DM, Salvatore DA, Reyes A, Huang A, Berlinguette CP: **Electrolytic CO_2 reduction in a flow cell**. *Acc Chem Res* 2018, **51**:910–918.

10. Qin B, Li Y, Wang H, Yang G, Cao Y, Yu H, Zhang Q, Liang H, Peng F: **Efficient electrochemical reduction of CO_2 into CO promoted by sulfur vacancies**. *Nano Energy* 2019, **60**:43–51.

11. Wei L, Li H, Chen J, Yuan Z, Huang Q, Liao X, Henkelman G, Chen Y: **Thiocyanate-modified silver nanofoam for efficient CO_2 reduction to CO**. *ACS Catal* 2020, **10**:1444–1453.

12. Piao G, Yoon SH, Han DS, Park H: **Ion-enhanced conversion of CO_2 into formate on porous dendritic bismuth electrodes with high efficiency and durability**. *ChemSusChem* 2020, **13**:698–706.

13. Díaz-Sainz G, Alvarez-Guerra M, Solla-Gullón J, García-Cruz L, Montiel V, Irabien A: **CO_2 electroreduction to formate: Continuous single-pass operation in a filter-press reactor at high current densities using Bi gas diffusion electrodes**. *J CO2 Util* 2019, **34**:12–19.

14. Sen S, Brown SM, Leonard M, Brushett FR: **Electroreduction of carbon dioxide to formate at high current densities using tin and tin oxide gas diffusion electrodes**. *J Appl Electrochem* 2019, **49**:917–928.

15. Guan A, Chen Z, Quan Y, Peng C, Wang Z, Sham T-K, Yang C, Ji Y, Qian L, Xu X, et al.: **Boosting CO_2 electroreduction to CH_4 via tuning neighboring single-copper sites**. *ACS Energy Lett* 2020, doi:10.1021/acsenergylett.0c00018.

16. Zhang T, Verma S, Kim S, Fister TT, Kenis PJA, Gewirth AA: **Highly dispersed, single-site copper catalysts for the electroreduction of CO_2 to methane**. *J Electroanal Chem* 2020, doi:10.1016/j.jelechem.2020.113862.

17. Hazarika J, Manna MS: **Electrochemical reduction of CO_2 to methanol with synthesized Cu_2O nanocatalyst: Study of the selectivity**. *Electrochimica Acta* 2019, **328**:135053.

18. Albo J, Beobide G, Castaño P, Irabien A: **Methanol electrosynthesis from CO_2 at Cu_2O/ZnO prompted by pyridine-based aqueous solutions**. *J CO2 Util* 2017, **18**:164–172.

19. Yuan J, Yang M-P, Zhi W-Y, Wang H, Wang H, Lu J-X: **Efficient electrochemical reduction of CO_2 to ethanol on Cu nanoparticles decorated on N-doped graphene oxide catalysts**. *J CO2 Util* 2019, **33**:452–460.

20. Su X, Sun Y, Jin L, Zhang L, Yang Y, Kerns P, Liu B, Li S, He J: **Hierarchically porous Cu/Zn bimetallic catalysts for highly selective CO_2 electroreduction to liquid C_2 products**. *Appl Catal B Environ* 2020, **269**:118800.

21. Gao Y, Wu Q, Liang X, Wang Z, Zheng Z, Wang P, Liu Y, Dai Y, Whangbo M-H, Huang B: **Cu_2O nanoparticles with both {100} and {111} facets for enhancing the selectivity and activity of CO_2 electroreduction to ethylene**. *Adv Sci* 2020, **7**:1902820.

22. Chou T-C, Chang C-C, Yu H-L, Yu W-Y, Dong C-L, Velasco-Vélez J-J, Chuang C-H, Chen L-C, Lee J-F, Chen J-M, et al.: **Controlling the oxidation state of the Cu electrode and reaction intermediates for electrochemical CO_2 reduction to ethylene**. *J Am Chem Soc* 2020, **142**:2857–2867.

23. Na J, Seo B, Kim J, Lee CW, Lee H, Hwang YJ, Min BK, Lee DK, Oh H-S, Lee U: **General technoeconomic analysis for electrochemical coproduction coupling carbon dioxide reduction with organic oxidation**. *Nat Commun* 2019, **10**:1–13.

24. Sánchez-Sánchez CM, Montiel V, Tryk DA, Aldaz A, Fujishima A: **Electrochemical approaches to alleviation of the problem of carbon dioxide accumulation**. *Pure Appl Chem* 2001, **73**:1917–1927.

25. Montiel MA, Solla-Gullón J, Montiel V, Sánchez-Sánchez CM: **Electrocatalytic studies on imidazolium based ionic liquids: Defining experimental conditions**. *Phys Chem Chem Phys* 2018, **20**:19160–19167.

26. Aránarán-Ais RM, Gao D, Roldan Cuenya B: **Structure-and electrolyte-sensitivity in CO_2 electroreduction**. *Acc Chem Res* 2018, **51**:2906–2917.

27. Sánchez-Sánchez CM: **Electrocatalytic reduction of CO_2 in imidazolium-based ionic liquids**. *Wandelt K Ed Encycl Interfacial Chem Surf Sci Electrochem* 2018, **5**:539–551.

28. Gao D, McCrum IT, Deo S, Choi YW, Scholten F, Wan W, Chen JG, Janik MJ, Roldan Cuenya B: **Activity and selectivity control in CO_2 electroreduction to multicarbon products over CuO_X catalysts via electrolyte design**. *ACS Catal* 2018, **8**:10012–10020.

29. Ross MB, Luna PD, Li Y, Dinh C-T, Kim D, Yang P, Sargent EH: **Designing materials for electrochemical carbon dioxide recycling**. *Nat Catal* 2019, **2**:648–658.

30. Merino-Garcia I, Alvarez-Guerra E, Albo J, Irabien A: **Electrochemical membrane reactors for the utilisation of carbon dioxide**. *Chem Eng J* 2016, **305**:104–120.

31. Vennekoetter J-B, Sengpiel R, Wessling M: **Beyond the catalyst: How electrode and reactor design determine the product spectrum during electrochemical CO_2 reduction**. *Chem Eng J* 2019, **364**:89–101.

32. Albo J, Vallejo D, Beobide G, Castillo O, Castaño P, Irabien A: **Copper-based metal–organic porous materials for CO_2 electrocatalytic reduction to alcohols**. *ChemSusChem* 2017, **10**:1100–1109.

33. Huo Y, Peng X, Liu X, Li H, Luo J: **High selectivity toward C_2H_4 production over Cu particles supported by butterfly-wing-derived carbon frameworks**. *ACS Appl Mater Interfaces* 2018, **10**:12618–12625.

34. Zhang F, Co AC: **Direct evidence of local pH change and the role of alkali cation during CO_2 electroreduction in aqueous media**. *Angew Chem Int Ed* 2019, doi:10.1002/anie.201912637.

35. Chae SY, Lee SY, Joo O-S: **Directly synthesized silver nanoparticles on gas diffusion layers by electrospray pyrolysis for electrochemical CO_2 reduction**. *Electrochimica Acta* 2019, **303**:118–124.

36. Luo W, Zhang J, Li M, Züttel A: **Boosting CO production in electrocatalytic CO_2 reduction on highly porous Zn catalysts**. *ACS Catal* 2019, **9**:3783–3791.

37. Pander JE, Lum JWJ, Yeo BS: **The importance of morphology on the activity of lead cathodes for the reduction of carbon dioxide to formate**. *J Mater Chem A* 2019, **7**:4093–4101.

38. Bohlen B, Wastl D, Radomski J, Sieber V, Vieira L: **Electrochemical CO_2 reduction to formate on indium catalysts prepared by electrodeposition in deep eutectic solvents**. *Electrochem Commun* 2020, **110**:106597.

39. Lai Q, Yuan W, Huang W, Yuan G: **Sn/SnO_x electrode catalyst with mesoporous structure for efficient electroreduction of CO_2 to formate**. *Appl Surf Sci* 2020, **508**:145221.

40. Feng D-M, Sun Y, Liu Z-Q, Zhu Y-P, Ma T-Y: **Designing nanostructured metal-based CO_2 reduction electrocatalysts**. 2019, doi:info:doi/10.1166/jnn.2019.16648.

41. Merino□Garcia I, Albo J, Irabien A: **Productivity and selectivity of gas-phase CO_2 electroreduction to methane at copper nanoparticle-based electrodes**. *Energy Technol* 2017, **5**:922–928.

42. Varela AS, Ju W, Reier T, Strasser P: **Tuning the catalytic activity and selectivity of Cu for CO_2 electroreduction in the presence of halides**. *ACS Catal* 2016, **6**:2136–2144.

43. Varela AS, Kroschel M, Reier T, Strasser P: **Controlling the selectivity of CO_2 electroreduction on copper: The effect of the electrolyte concentration and the importance of the local pH**. *Catal Today* 2016, **260**:8–13.

44. Reske R, Mistry H, Behafarid F, Roldan Cuenya B, Strasser P: **Particle size effects in the catalytic electroreduction of CO_2 on Cu nanoparticles**. *J Am Chem Soc* 2014, **136**:6978–6986.

45. Dinh C-T, Burdyny T, Kibria MG, Seifitokaldani A, Gabardo CM, Arquer FPG de, Kiani A, Edwards JP, Luna PD, Bushuyev OS, et al.: **CO_2 electroreduction to ethylene via hydroxide-mediated copper catalysis at an abrupt interface**. *Science* 2018, **360**:783–787.

46. Lum Y, Yue B, Lobaccaro P, Bell AT, Ager JW: **Optimizing C-C coupling on oxide-derived copper catalysts for electrochemical CO_2 reduction**. *J Phys Chem C* 2017, **121**:14191–14203.

47. Lee SY, Jung H, Kim N-K, Oh H-S, Min BK, Hwang YJ: **Mixed copper states in anodized Cu electrocatalyst for stable and selective ethylene production from CO_2 reduction**. *J Am Chem Soc* 2018, **140**:8681–8689.

48. Pander III JE, Ren D, Huang Y, Loo NWX, Hong SHL, Yeo BS: **Understanding the heterogeneous electrocatalytic reduction of carbon dioxide on oxide-derived catalysts**. *ChemElectroChem* 2018, **5**:219–237.

49. Grosse P, Gao D, Scholten F, Sinev I, Mistry H, Roldan Cuenya B: **Dynamic changes in the structure, chemical state and catalytic selectivity of Cu nanocubes during CO_2 electroreduction: size and support effects**. *Angew Chem Int Ed* 2018, **57**:6192–6197.

50. Varela AS, Ju W, Bagger A, Franco P, Rossmeisl J, Strasser P: **Electrochemical reduction of CO_2 on metal-nitrogen-doped carbon catalysts**. *ACS Catal* 2019, **9**:7270–7284.

51. Li A, Nicolae SA, Qiao M, Preuss K, Szilágyi PA, Moores A, Titirici M: **Homogenous meets heterogenous and electro□catalysis: iron□nitrogen molecular complexes within carbon materials for catalytic applications**. *ChemCatChem* 2019, **11**:3602–3625.

52. Roy A, Hursán D, Artyushkova K, Atanassov P, Janáky C, Serov A: **Nanostructured metal-N-C electrocatalysts for CO_2 reduction and hydrogen evolution reactions**. *Appl Catal B Environ* 2018, **232**:512–520.

53. Zúñiga C, Candia-Onfray C, Venegas R, Muñoz K, Urra J, Sánchez-Arenillas M, Marco JF, Zagal JH, Recio FJ: **Elucidating the mechanism of the oxygen reduction reaction for pyrolyzed Fe-N-C catalysts in basic media**. *Electrochem Commun* 2019, **102**:78–82.

54. Leonard ND, Wagner S, Luo F, Steinberg J, Ju W, Weidler N, Wang H, Kramm UI, Strasser P: **Deconvolution of utilization, site density, and turnover frequency of Fe–Nitrogen–Carbon oxygen reduction reaction catalysts prepared with secondary n-precursors**. *ACS Catal* 2018, **8**:1640–1647.

55. Varela AS, Ranjbar Sahraie N, Steinberg J, Ju W, Oh H-S, Strasser P: **Metal-doped nitrogenated carbon as an efficient catalyst for direct CO_2 electroreduction to CO and hydrocarbons**. *Angew Chem Int Ed* 2015, **54**:10758–10762.

56. Pan F, Deng W, Justiniano C, Li Y: **Identification of champion transition metals centers in metal and nitrogen-codoped carbon catalysts for CO_2 reduction**. *Appl Catal B Environ* 2018, **226**:463–472.

57. Li J, Pršlja P, Shinagawa T, Martín Fernández AJ, Krumeich F, Artyushkova K, Atanassov P, Zitolo A, Zhou Y, García-Muelas R, et al.: **Volcano trend in electrocatalytic CO_2 reduction activity over atomically dispersed metal sites on nitrogen-doped carbon**. *ACS Catal* 2019, **9**:10426–10439.

58. Hu X-M, Hval HH, Bjerglund ET, Dalgaard KJ, Madsen MR, Pohl M-M, Welter E, Lamagni P, Buhl KB, Bremholm M, et al.: **Selective CO_2 reduction to CO in water using earth-abundant metal and nitrogen-doped carbon electrocatalysts**. *ACS Catal* 2018, **8**:6255–6264.

59. Varela AS, Kroschel M, Leonard ND, Ju W, Steinberg J, Bagger A, Rossmeisl J, Strasser P: **PH effects on the selectivity of the electrocatalytic CO_2 reduction on graphene-embedded Fe–N–C motifs: bridging concepts between molecular homogeneous and solid-state heterogeneous catalysis**. *ACS Energy Lett* 2018, **3**:812–817.

60. Jiang K, Siahrostami S, Zheng T, Hu Y, Hwang S, Stavitski E, Peng Y, Dynes J, Gangisetty M, Su D, et al.: **Isolated Ni single atoms in graphene nanosheets for high-performance CO_2 reduction**. *Energy Environ Sci* 2018, **11**:893–903.

61. Daems N, Mot BD, Choukroun D, Daele KV, Li C, Hubin A, Bals S, Hereijgers J, Breugelmans T: **Nickel-containing N-doped carbon as effective electrocatalysts for the reduction of CO_2 to CO in a continuous-flow electrolyzer**. *Sustain Energy Fuels* 2019, doi:10.1039/C9SE00814D.

62. Nitopi S, Bertheussen E, Scott SB, Liu X, Engstfeld AK, Horch S, Seger B, Stephens IEL, Chan K, Hahn C, et al.: **Progress and perspectives of electrochemical CO_2 reduction on copper in aqueous electrolyte**. *Chem Rev* 2019, **119**:7610–7672.

63. Mistry H, Varela AS, Bonifacio CS, Zegkinoglou I, Sinev I, Choi Y-W, Kisslinger K, Stach EA, Yang JC, Strasser P, et al.: **Highly selective plasma-activated copper catalysts for carbon dioxide reduction to ethylene**. *Nat Commun* 2016, **7**:1–9.

64. Qiao J, Liu Y, Hong F, Zhang J: **A review of catalysts for the electroreduction of carbon dioxide to produce low-carbon fuels**. *Chem Soc Rev* 2014, **43**:631–675.

65. Smith BD, Irish DE, Kedzierzawski P, Augustynski J: **A surface enhanced roman scattering study of the intermediate and poisoning species formed during the electrochemical reduction of CO_2 on copper**. *J Electrochem Soc* 1997, **144**:4288.

66. Frese KW: **Electrochemical reduction of CO_2 at intentionally oxidized copper electrodes**. *J Electrochem Soc* 1991, **138**:3338–3344.

67. Cheng Y-S, Li H, Ling M, Li N, Jiang B, Wu F-H, Yuan G, Wei X-W: **Synthesis of Cu_2O@Cu-Fe-K Prussian Blue analogue core–shell nanocube for enhanced electroreduction of CO_2 to multi-carbon products**. *Mater Lett* 2020, **260**:126868.

68. Qi L, Liu S, Gao W, Jiang Q: **Mechanistic understanding of CO_2 electroreduction on Cu_2O**. *J Phys Chem C* 2018, **122**:5472–5480.

69. Chen C, Sun X, Lu L, Yang D, Ma J, Zhu Q, Qian Q, Han B: **Efficient electroreduction of CO_2 to C_2 products over B-doped oxide-derived copper**. *Green Chem* 2018, **20**:4579–4583.

70. Merino-Garcia I, Albo J, Solla-Gullón J, Montiel V, Irabien A: **Cu oxide/ZnO-based surfaces for a selective ethylene production from gas-phase CO_2 electroconversion**. *J CO2 Util* 2019, **31**:135–142.

71. Yang H-J, Yang H, Hong Y-H, Zhang P-Y, Wang T, Chen L-N, Zhang F-Y, Wu Q-H, Tian N, Zhou Z-Y, et al.: **Promoting ethylene selectivity from CO_2 electroreduction on CuO supported onto CO_2 capture materials**. *ChemSusChem* 2018, **11**:881–887.

72. Wang W, Ning H, Yang Z, Feng Z, Wang J, Wang X, Mao Q, Wu W, Zhao Q, Hu H, et al.: **Interface-induced controllable synthesis of Cu_2O nanocubes for electroreduction CO_2 to C_2H_4**. *Electrochimica Acta* 2019, **306**:360–365.

73. Jung H, Lee SY, Lee CW, Cho MK, Won DH, Kim C, Oh H-S, Min BK, Hwang YJ: **Electrochemical fragmentation of Cu_2O nanoparticles enhancing selective C–C coupling from CO_2 reduction reaction**. *J Am Chem Soc* 2019, **141**:4624–4633.

74. Lum Y, Ager JW: **Stability of residual oxides in oxide-derived copper catalysts for electrochemical CO_2 reduction investigated with ^{18}O labeling**. *Angew Chem Int Ed* 2018, **57**:551–554.

75. Xiang H, Rasul S, Scott K, Portoles J, Cumpson P, Yu EH: **Enhanced selectivity of carbonaceous products from electrochemical reduction of CO_2 in aqueous media**. *J CO2 Util* 2019, **30**:214–221.

76. Ren D, Fong J, Yeo BS: **The effects of currents and potentials on the selectivities of copper toward carbon dioxide electroreduction**. *Nat Commun* 2018, **9**:925 doi:10.1038/s41467-018-03286-w.

77. Lum Y, Ager JW: **Evidence for product-specific active sites on oxide-derived Cu catalysts for electrochemical CO_2 reduction**. *Nat Catal* 2019, **2**:86–93.

78. Chen Y, Zou L, Liu H, Chen C, Wang Q, Gu M, Yang B, Zou Z, Fang J, Yang H: **Fe and N co-doped porous carbon nanospheres with high density of active sites for efficient CO_2 electroreduction**. *J Phys Chem C* 2019, **123**:16651–16659.

79. Qin X, Zhu S, Xiao F, Zhang L, Shao M: **Active sites on heterogeneous single-iron-atom electrocatalysts in CO_2 reduction reaction**. *ACS Energy Lett* 2019, **4**:1778–1783.

80. Yang H-J, Zhang X, Hong Y-H, Sari HMK, Zhou Z-Y, Sun S-G, Li X-F: **Superior selectivity and tolerance towards metal-ion impurities of a Fe/N/C catalyst for CO_2 reduction**. *ChemSusChem* 2019, **12**:3988–3995.

81. Pan F, Li B, Sarnello E, Hwang S, Gang Y, Feng X, Xiang X, Adli NM, Li T, Su D, et al.: **Boosting CO_2 reduction on Fe-N-C with sulfur incorporation: synergistic electronic and structural engineering**. *Nano Energy* 2020, **68**:104384.

82. Wang Z-L, Choi J, Xu M, Hao X, Zhang H, Jiang Z, Zuo M, Kim J, Zhou W, Meng X, et al.: **Optimizing electron densities of Ni-N-C complexes by hybrid coordination for efficient electrocatalytic CO_2 reduction**. *ChemSusChem* 2020, **13**:929–937.

83. Zhang M, Wu T-S, Hong S, Fan Q, Soo Y-L, Masa J, Qiu J, Sun Z: **Efficient electrochemical reduction of CO_2 by Ni–N catalysts with tunable performance**. *ACS Sustain Chem Eng* 2019, **7**:15030–15035.

84. Ma S, Su P, Huang W, Jiang SP, Bai S, Liu J: **Atomic Ni species anchored N-doped carbon hollow spheres as nanoreactors for efficient electrochemical CO_2 reduction**. *ChemCatChem* 2019, **11**:6092–6098.

85. Fan Q, Hou P, Choi C, Wu T-S, Hong S, Li F, Soo Y-L, Kang P, Jung Y, Sun Z: **Activation of Ni particles into single Ni–N atoms for efficient electrochemical reduction of CO_2**. *Adv Energy Mater* 2019, doi:10.1002/aenm.201903068.

86. Pan F, Zhang H, Liu Z, Cullen D, Liu K, More K, Wu G, Wang G, Li Y: **Atomic-level active sites of efficient imidazolate framework-derived nickel catalysts for CO_2 reduction**. *J Mater Chem A* 2019, **7**:26231–26237.

Table 1. Comparison of the performance of different OD-Cu catalysts recently reported in literature for CO_2RR.

Fig. 1 (a) Schematic presentation of CO_2 electroreduction to C_2H_4 on interface-induced method to prepare Cu_2O nanocubes on ionic liquid functionalized graphite sheets. Reprinted with permission from ref [72]. Copyright 2019 Elsevier. (b) HRTEM image for Cu based nanoparticles after 10 h of CO_2RR. Adapted with permission from ref [73]. Copyright 2019 American Chemical Society. (c) (d) (e) Faradaic efficiency of methane, ethylene and ethanol, carbon monoxide and formate on different catalysts at different potentials, respectively. Different catalysts Cu-10, CuO-1, CuO-10, and CuO-60 are Cu based catalysts electrodeposited for 1 min, 10 min and 60 min, respectively, which are shown in color of orange, green, red and blue, respectively. Error bars in (c)–(e) represent the standard deviations of three independent measurements. Open access article ref [76]. Distributed under the terms of the Creative Commons CC BY license.

Fig. 2 (a) General synthesis strategy of M-N-C catalysts and their obtained structure. Reprinted with permission from ref [50]. Copyright 2019 American Chemical Society. (b) CO FEs at different metal-N-C catalysts. Reprinted with permission from ref [56]. Copyright 2018 Elsevier. (c) LSV curves of Fe−N−PC, op−Fe−N−PC and N−PC in CO_2-saturated 0.5 $mol \cdot L^{-1}$ $KHCO_3$ solution (scan rate = 10 mV/s). Reprinted with permission from ref [78]. Copyright 2019 American Chemical Society. (d) Gibbs free energy diagrams of CO_2RR on different sites by DFT. Reprinted with permission from ref [79]. Copyright 2019 American Chemical Society (e) S doped Fe-M-C structure. (f) Comparison of FEs to CO in 0.1 M $KHCO_3$ aqueous solution on different catalysts. Reprinted with permission from ref [81]. Copyright 2019 Elsevier.

Fig.3 (a) Free energy diagram of CO_2RR to CO on $Ni@N_4$, $Ni@N_3$ (pyrrolic) and $Ni@N_3$ (pyridinic). Reprinted with permission from ref [85]. Copyright 2019 John Wiley and Sons. (b) CO and H_2 Faradaic efficiency and (c) CO partial current density for N–C and Ni–N–C. (d) Initial and final states for the COOH dissociation reaction on $Ni–N_4–C_{10}$ and $Ni–N_{2+2}–C_8$ sites. Reprinted with permission from ref [86]. Copyright 2019 Royal Society of Chemistry.

Table 1.

OD-Cu catalysts	Electrolyte	E / V vs. RHE	Target products	FE (%)	Ref
Cu_2O NP	$KHCO_3$	-2.0 V vs. SHE	CH_3OH	47.5	[17]
Cu_2O@K-PBA	n.a.	-1.11	C_2H_4	23.9	[67]
B-OD Cu	0.1 M $KHCO_3$	-1.05	C_2	48.2	[69]
Cu oxides/ZnO	0.1 M $KHCO_3$	-2.5 V vs. Ag/AgCl	C_2H_4	91.1	[70]
CuO/N_xC	0.1 M $NaHCO_3$	-1.25	C_2H_4	36	[71]
Cu_2O/ILGS	0.1 M $KHCO_3$	-1.15	C_2H_4	31.1	[72]
Cu_2O NP/C	0.1 M $KHCO_3$	-1.1	C_2/C_3	74	[73]
OD Cu	0.1 M $KHCO_3$	-1.0	C_2/C_3	60	[74]
Cu_xO	2.0 M KOH	-1.17	C_2	40	[75]
Different OD Cu	0.1 M $KHCO_3$	-0.9 ~ -1.1	C_2	48	[76]
		-1.15	CH_4	40	
		-0.5	CO	46	
		-0.6	$HCOO^-$	35	

Abbreviations: Nanoparticles (NP), Prussian Blue Analogue (PBA), B-OD (Boron-doped oxide-derived) and Ionic Liquid functionalized Graphite Sheets (ILGS).

Fig.1

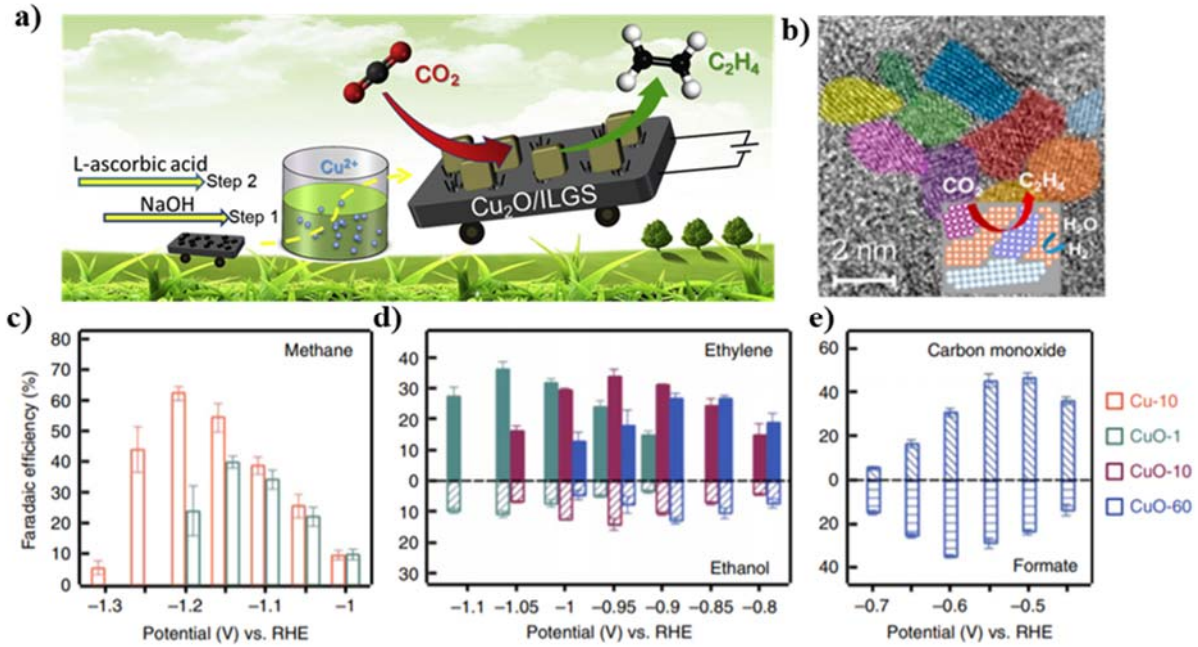
a)
CO2
C2H4
L-ascorbic acid
Step 2
NaOH
Step 1
Cu2+
Cu2O/ILGS
b)
CO2
C2H4
H2O
H2
2 nm
c)
Methane
Faradaic efficiency (%)
Potential (V) vs. RHE
d)
Ethylene
Ethanol
Potential (V) vs. RHE
e)
Carbon monoxide
Formate
Potential (V) vs. RHE
Cu-10
CuO-1
CuO-10
CuO-60

Fig.2.

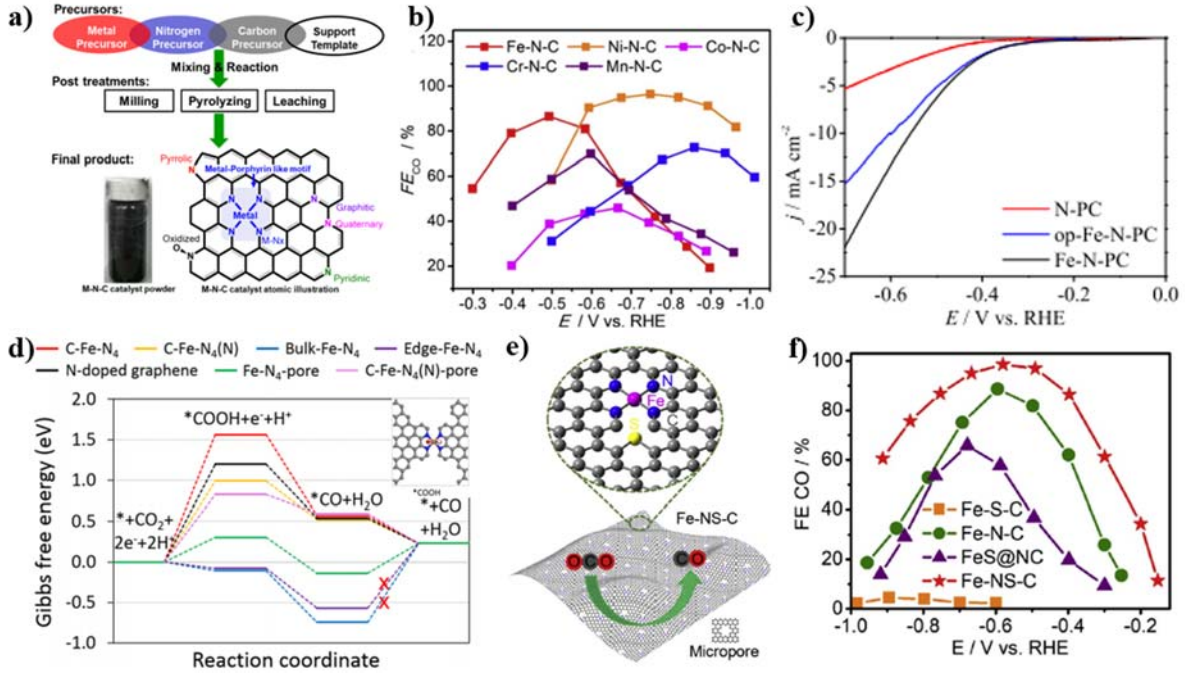
a)
Precursors:
Metal Precursor
Nitrogen Precursor
Carbon Precursor
Support Template
Mixing & Reaction
Post treatments:
Milling
Pyrolyzing
Leaching
Final product:
Pyrrolic
Metal-Porphyrin like motif
Graphitic
N-Quaternary
Oxidized
M-Nx
Pyridinic
M-N-C catalyst powder
M-N-C catalyst atomic illustration
b)
Fe-N-C
Ni-N-C
Co-N-C
Cr-N-C
Mn-N-C
FE_CO / %
E / V vs. RHE
c)
j / mA cm^-2
N-PC
op-Fe-N-PC
Fe-N-PC
E / V vs. RHE
d)
C-Fe-N4
C-Fe-N4(N)
Bulk-Fe-N4
Edge-Fe-N4
N-doped graphene
Fe-N4-pore
C-Fe-N4(N)-pore
Gibbs free energy (eV)
*COOH+e-+H+
*+CO2+ 2e-+2H+
*CO+H2O
*+CO +H2O
Reaction coordinate
e)
Fe-NS-C
Micropore
f)
FE CO / %
Fe-S-C
Fe-N-C
FeS@NC
Fe-NS-C
E / V vs. RHE

Fig.3.

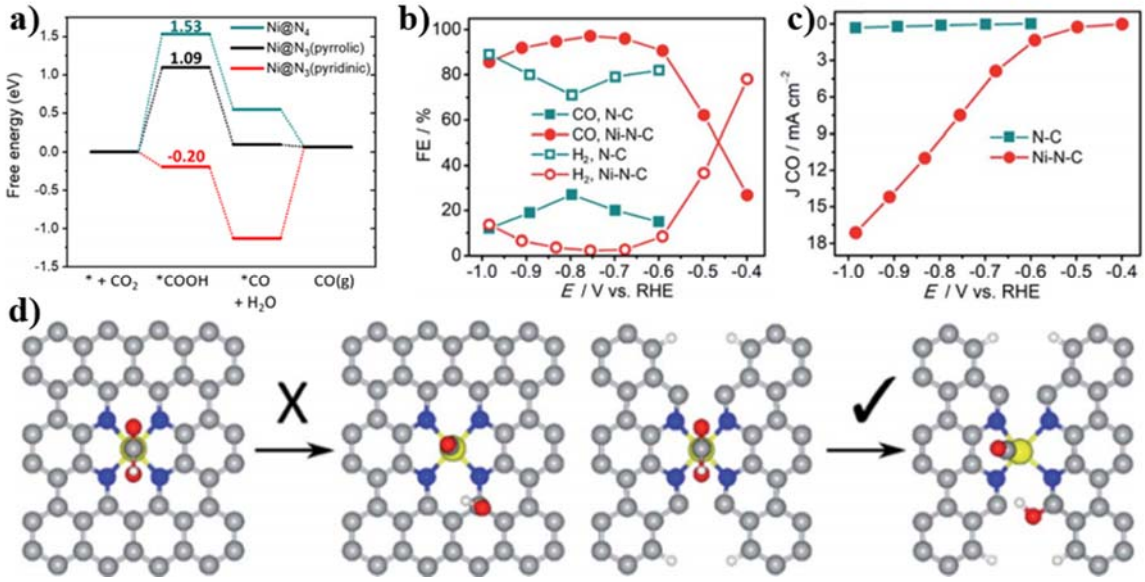
a)
Free energy (eV)
1.53
1.09
-0.20
Ni@N4
Ni@N3(pyrrolic)
Ni@N3(pyridinic)
* + CO2
*COOH
*CO
+ H2O
CO(g)
b)
FE / %
CO, N-C
CO, Ni-N-C
H2, N-C
H2, Ni-N-C
E / V vs. RHE
c)
J CO / mA cm-2
N-C
Ni-N-C
E / V vs. RHE
d)
X
✓

Appendix

Papers of particular interest, published within the period of review, have been highlighted as:

* of special interest

** of outstanding interest

*[5]	This review comprehensively summarized metal–organic complexes, metals, metal alloys, inorganic metal compounds and carbon-based metal-free nanomaterials for CO_2 reduction.
*[27]	Different abbreviation systems for denoting imidazolium-based room temperature ionic liquids (RTILs) used for CO_2 electrochemical conversion are reviewed about their physicochemical properties.
**[50]	This review analyzed various factors and described DFT directing experiments on the activity and selectivity of M-N-Cs.
**[60]	This paper strengthened the importance of single atoms Ni for CO_2RR in several aspects and demonstrated different performance of various Ni active sites.
**[71]	This paper described cubic Cu_2O crystalline particles electrochemically fragmentate into smaller particles and the grain boundaries generated can promote C-C coupling in CO_2RR.
**[72]	This article demonstrated faster oxygen diffusion and oxide nucleation in Cu oxides catalyst for Cu reoxidation on grain boundaries.
**[74]	The authors illustrated products selectivity relies on surface roughness and revealed the effects of applied potential on the products selectivity of CO_2RR.
**[80]	This paper showed an outstanding Faradaic efficiency (99%) for CO and studied the stable catalytic performance of the Fe-N-CSCN even with the addition of metal-ion impurities because of the numerous separated active sites.
*[81]	This paper proved the dopant sulfur in Fe-N-C structure can enhance the Faradaic efficiency to CO (98%).
**[86]	This paper adopted DFT calculation to compare the active sites of Ni-N_4-C_{10} and Ni-N_{2+2}-C_8 and found that the edge-located Ni-N_{2+2}-C_8 are responsible for the good performance of CO_2RR because of lower free energy.